CEAS Aeronautical Journal (2022) 13:797–808
https://doi.org/10.1007/s13272-022-00592-4

ORIGINAL PAPER

Semi-analytical estimation of Helmholtz resonators' tuning frequency for scalable neck-cavity geometric couplings

Giuseppe Catapane[1] · Dario Magliacano[1,2] · Giuseppe Petrone[1,2] · Alessandro Casaburo[2] · Francesco Franco[1,2] · Sergio De Rosa[1,2]

Received: 29 March 2022 / Revised: 26 May 2022 / Accepted: 1 June 2022 / Published online: 1 July 2022

Abstract
Innovative meta-materials offer great flexibility for manipulating sound waves and assure unprecedented functionality in the context of acoustic applications. Indeed, they can exhibit extraordinary properties, such as broadband low-frequency absorption, excellent sound insulation, or enhanced sound transmission. These amazing properties have drawn the eye of the transport industry, especially for aeronautic applications where objects like these can be combined and coupled with primary structures aiming to reduce exterior and interior noise without increasing weight. However, the design of acoustic meta-materials with exciting functionality still represents a challenge, therefore there is a huge interest about the conceptualization and design of innovative acoustic solutions making use of meta-material resonance effects. The main target of the present research work is to obtain an accurate prediction of the tuning frequency of a Helmholtz-resonating device, whose resonance properties are exploited in a wide part of acoustic meta-material design. In this context, an investigation on a correction factor for the classical formulation used to estimate the Helmholtz resonance frequency starting from its geometric characteristics, accounting for different-shaped resonators with varying neck/cavity ratios, is performed. More specifically, a set of numerical simulations for several geometric configuration is considered in order to demonstrate the limits of pre-existing formulas, and a new correction factor formula is developed after theoretical considerations where it is possible. In the end, results in terms of correction factors are provided in both graphical and semi-analytical form, compared with Finite Element data.

Keywords Acoustics · Meta-material · Helmholtz · Resonator

✉ Giuseppe Catapane
giuseppe.catapane@unina.it

Dario Magliacano
dario.magliacano@unina.it

Giuseppe Petrone
giuseppe.petrone@unina.it

Alessandro Casaburo
alessandro.casaburo@wavesetconsulting.com

Francesco Franco
francesco.franco@unina.it

Sergio De Rosa
sergio.derosa@unina.it

[1] PASTA-Lab (Laboratory for Promoting experiences in Aeronautical STructures and Acoustics), Department of Industrial Engineering - Aerospace Section, Università degli Studi di Napoli "Federico II, Via Claudio 21, 80125 Naples, Italy

[2] WaveSet S.R.L., Via A. Gramsci 15, 80122 Naples, Italy

1 Introduction

Nowadays transport industry has to cope several not-trivial problems without affecting performance of the present models and/or relative costs. One of the most important is surely noise disturbance produced by each structure that vibrates. For instance, an aircraft design procedure cannot neglect sound emission considerations, and an aircraft which is too noisy will never be sold or certified. On the other hand, a sound suppression system should be as light as possible and placed in established and very limited spaces. It is easy to understand that conventional solutions are not accountable for transport field applications, above all for the aeronautic industry. Acoustic meta-materials are introduced to successfully overcome these severe transport boundary conditions [1, 2]; their design is based on substructures that, if correctly shaped and arranged, can perform a robust sound absorption or suppression [3], also compared to active-controlled solutions [4]. Aiming at this goal, different objects could

be investigated and adopted in order to consider them as a unit cell of the acoustic meta-material: for example, porous media, whose foam cavities dissipate the energy by viscous and thermal losses [5], show very good performance at high frequencies [6], while tunable acoustic devices, such as Helmholtz resonators (HRs), perform better at low frequencies.

The concept of Helmholtz resonance and the associated classical theory have been applied in the design and analysis of various systems, including: tuned intake manifolds of vehicles [7–9], noise attenuation in pipelines [10], attenuation of aircraft propeller noise [11], combustion instabilities for gas-turbine engines [12]. With reference to this class of devices, Alster [13] obtained the classical formula for calculation of resonant frequencies of HRs, under the assumptions that all mass significant for oscillation of a resonator is concentrated in the neck of the resonator and that the spring constant is given by the volume of the resonator [14]. Tang et al. [15] derived the theory of a generalized HR, based on the jet-flow model that is manifested in the non-linearity of the neck flow upon the passage of a high intensity wave. Fahy et al. [16] coupled a single HR to an enclosure and tuned it to the natural frequency of one of its low order acoustic modes, also analyzing the effect on the free, and forced, vibrations of the fluid in the enclosure. Chanaud [17] developed an equation for the resonance frequency of a HR from the wave equation for the case of a cavity volume that has the shape of a cuboid and orifices of different geometries. de Bedout et al. [18] presented a tunable Helmholtz resonator and a feedback-based control law that achieves optimal resonator tuning for time-varying tonal noise control applications. Lei et al. [19] proposed a strategy to characterize power and ground-plane structures using a full cavity-mode frequency-domain resonator model. Griffin et al. [20] demonstrated that mechanically coupled resonators can be used for designing a particular transmission loss response, generating attenuation in a wider bandwidth, and adapting the transmission loss characteristics of a structure to attenuate disturbances at a desired frequency. Tang [21] experimentally and theoretically investigated the acoustical properties of HRs with necks having cross-section dimensions decreasing away from the entry of the resonator cavities. Park [22] introduced micro-perforated panel absorbers backed by HRs with the aim to improve sound absorption in the low-frequency range, where classical micro-perforated panel absorbers do not provide sufficient performance. As a consequence, HRs are analyzed by several researcher for their interesting behavior; apparently, these ones do not change with the HR shape. Nevertheless, resonance frequency prediction formulas are not so much faithful for shapes that are different respect to those that are typically analyzed in literature (e.g.: cylinder neck - cylinder cavity); furthermore, a classic geometry like cylinder neck - cylinder cavity can have a different resonance frequency shift depending on the radii ratios. The scope of this paper is to obtain an accurate prediction of the tuning frequency of a HR device, for several combination of neck-cavity geometries. In detail, the present manuscript wants to further improve the results already obtained by Catapane et al. [23], by taking into account the limits of the polynomial resonance prediction and proving that a new semi-analytical approach can overcome this problem for specific geometries.

The present work is structured as follows: in Sect. 2, Helmholtz resonators are thoroughly introduced, together with some details about geometric properties 2.1) and Finite Element (FE) implementation (Sect. 2.2). Successively, in Sect. 3, the correction factor study is herein presented and discussed, with the introduction of a graphical-polynomial method for the resonance frequency estimation (Sect. 3.1), showing the main advantages and drawbacks of the current approach (Sect. 3.2). Subsequently, in Sect. 4, the semi-analytical estimation is described, with its methodological framework (Sect. 4.1), and the discussion of its results (Sect. 4.2). In conclusion, in Sect. 5, the main achievements of the present research are summarized and some possible future expansions are identified.

2 Definition of the problem

A Helmholtz resonator (HR) is a tunable device with rigid walls and filled of fluid, whose geometry is usually represented by a neck followed by a cavity. With reference to acoustic applications, HRs exhibit a single resonance frequency; thus, they are commonly defined as 1-Degree-of-Freedom (DoF) systems. Indeed, HR may be conceptually assimilated to a mass-spring system, in which the the volume acts as a spring, and the fluid in the neck represents the mass, with expressions which are respectively:

$$K = \rho_0 c_0^2 S_{\text{neck}}^2 / V_{\text{cavity}}, \tag{1a}$$

$$M = \rho_0 S_{\text{neck}} l_{\text{neck}}, \tag{1b}$$

where ρ_0 is the density of the fluid, c_0 is the speed of sound in the fluid, S_{neck} is the area of the section of the neck, V_{cavity} is the volume of the cavity, and l_{neck} is the main length of the neck. In detail, the stiffness expression can be determined by considering a piston inside the neck pushed of a cyan$\bar{x}$ quantity: the volume of the cavity is consequently changed of a quantity $\Delta V_{cavity} = -S_{neck}\bar{x}$, resulting in a condensation $\Delta\rho/\rho = \Delta V/V = S\bar{x}/V$ and hence a pressure increase $p = \rho c^2 \Delta\rho/\rho = \rho_0 c^2 S_{neck}\bar{x}/V_{cavity}$ As a consequence, the force against this displacement is $F = pS_{neck} = K\bar{x}$ with K having the expression of Eq. 1a. Furthermore, the radiation mass must be considered as the mass of the fluid contained

in the neck plus a $\Delta V = S_{neck}\Delta L$ due to connection between neck and cavity. The mass expression of Eq. 1b will be hence changed by considering the effective length $L_{eff} = l_{neck} + \Delta L$:

$$M = \rho_0 S_{\text{neck}} L_{\text{eff}}. \tag{2}$$

The equation of the inward displacement $\bar{x}$ for a Helmholtz Resonator can be written as:

$$M\frac{d^2\bar{x}}{dt^2} + K\bar{x} = fe^{i\omega t}, \tag{3}$$

with $fe^{i\omega t} = S_{\text{neck}} P e^{i\omega t}$ the instantaneous complex driving force produced by a pressure wave of amplitude P impinging on the device neck. It is easy to derive the natural frequency of the system as:

$$f_{res} = \frac{c_0}{2\pi}\sqrt{\frac{S_{\text{neck}}}{V_{\text{cavity}} L_{\text{eff}}}}. \tag{4}$$

The resistance of the system is neglected, assuming that this term has no meaningful effect on the resonance frequency of the system in the case of rigid walls or materials that are generally used for the fabrication of such a device. Furthermore, the theory herein reported can be more extensively investigated in the books of Kinsler [14] and Long [24]. Eq. 4 can be easily solved by knowing the geometric properties of the Helmholtz Resonator, except for L_{eff}, which needs more considerations. The first length correction for a HR tuning frequency $f_{res(Rayleigh)}$ was proposed by Rayleigh [25] as:

$$f_{\text{res(Rayleigh)}} = \frac{c_0}{2\pi}\sqrt{\frac{S_{\text{neck}}}{V_{\text{cavity}}(l_{\text{neck}} + \frac{4}{3\pi}d_{\text{neck}})}}, \tag{5}$$

where $(4/3\pi)d_{neck}$ is an end-correction introduced for accounting neck-cavity junction effects due to an abrupt change between the circular cross sections. This change leads to an additional impedance, defined as discontinuity inductance. The physical phenomenon is well explained by Karal [26], who relates the discontinuity inductance to the ratio between the tube radii. This additional impedance can be conceptually interpreted as an increase in the length of the tube; moreover, if the ratio of the tube radii is unitary, the circular section is unchanged and thus the length does not need any corrections; on the other hand, for a ratio equal to zero (an open tube fitted with an infinite flange), the correction factor corresponds to the Rayleigh's one. Thus, it is logical that Rayleigh's correction works well for low value of tube radii ratio, while it needs further considerations when the ratio is increasing.

Successively, Ingard [27] modified Rayleigh's formula by increasing its complexity in order to provide an alternative estimation of HR frequency, which has explicit dependence on ξ, defined as the ration between the representative lengths in the section plane of the neck and the cavity, respectively labeled as d_{neck} and d_{cavity}:

$$\xi = d_{\text{neck}}/d_{\text{cavity}}. \tag{6}$$

Ingard developed this approach for three geometric configurations (cylindrical neck and cylindrical cavity, cylindrical neck and cuboid cavity, cuboid neck and cuboid cavity). Analogously to Ingard's approach, also Rayleigh's formula can be written by outlining its dependence from ξ, in the form of:

$$f_{\text{res}(\xi,\text{Rayleigh})} = \frac{c_0}{2\pi}\sqrt{\frac{S_{\text{neck}}}{V_{\text{cavity}} l_{\text{neck}}(1 + \frac{4}{3\pi}\frac{d_{\text{cavity}}}{l_{\text{neck}}}\xi)}}. \tag{7}$$

Finite Elements results demonstrate that Rayleigh's and Ingard's estimations perform well in a limited range of ξ, while sensibly differing from FE results for values of ξ outside of it. Thus, a new empirical prediction of HR frequency is developed herein, with the aim of obtaining a more accurate evaluation compared with those already available in the relevant literature. This is done starting from Eq. 7, and investigating the correction factor c_f, which plays the role defined as follows:

$$f_{res(\xi)} = \frac{c_0}{2\pi}\sqrt{\frac{S_{\text{neck}}}{V_{\text{cavity}} l_{\text{neck}}(1 + c_f\xi)}}. \tag{8}$$

The objective of the present work is to extend the results obtained and presented at the CEAS Aerospace Europe Conference 2021 by Catapane et al. [23]; thus, a part of the work is an improvement of the previous paper, where important details are modified, and necessary considerations about limits of the polynomial-graphical approach are discussed; the last part, instead, introduces a semi-analytical approach for the geometric couplings in order to further improve the previous correction factor estimation method. The latter method deletes completely scalability limits.

2.1 Geometric properties

Six different geometric configurations are considered herein (Fig. 1). A summary of the studied configurations is reported in Table 1 with a precise explanation of the characteristic lengths of necks and cavities for the studied configurations. As shown in the sub-figures and the table description, configurations with cuboid shape have a square surface area, but the same approach can be easily extended to even more complex geometries.

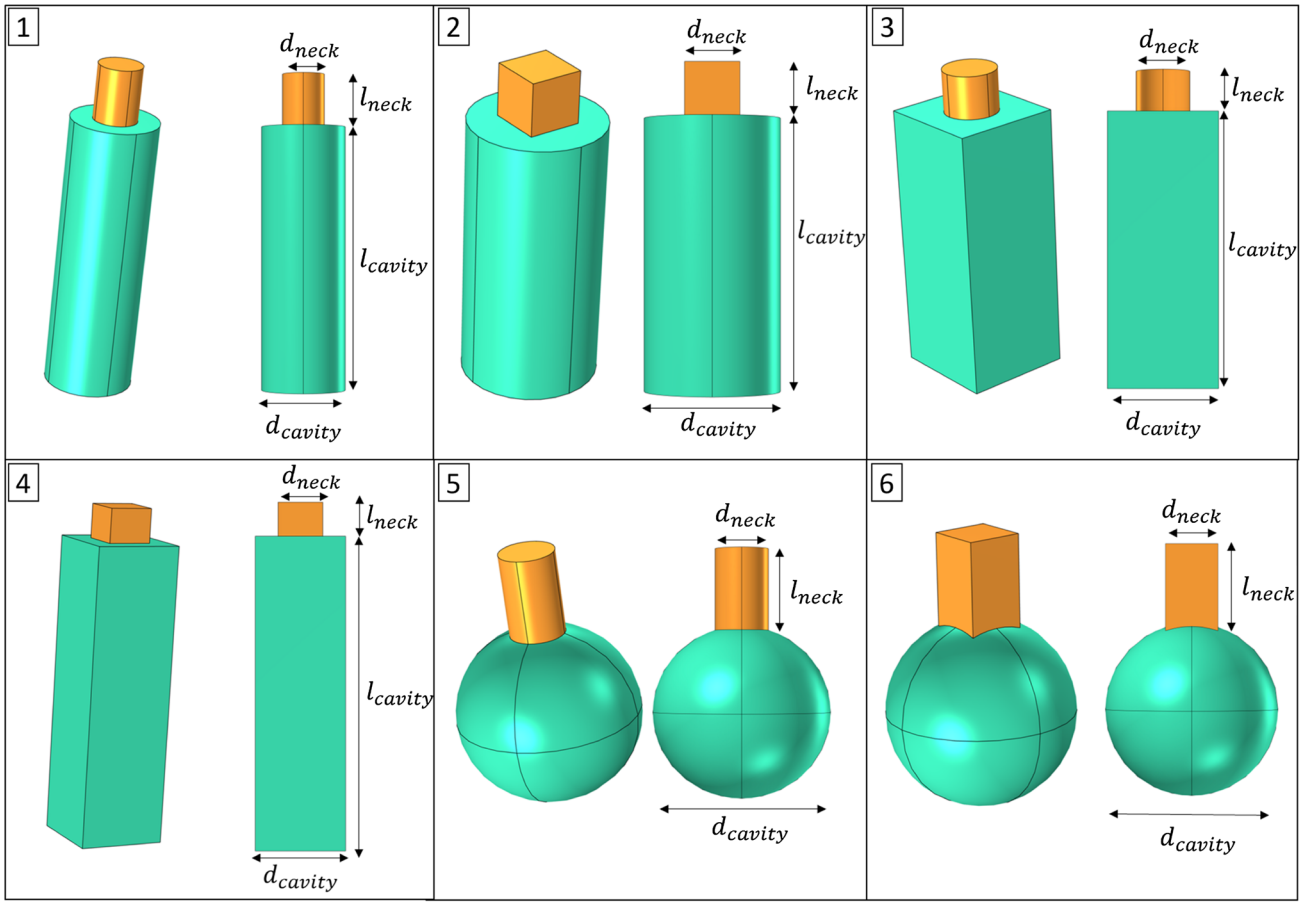

Fig. 1 Representation of the studied configurations, numbered as indicated in Table 1

Table 1 Characteristic lengths of necks and cavities for six different geometric configurations, where $\xi = d_{neck}/d_{cavity}$

C.	Neck Shape	Cavity Shape	d_{neck}	d_{cavity}
1	Cylinder	Cylinder	Diameter of the cylinder	Diameter of the cylinder
2	Cuboid	Cylinder	Length of the square base of the cuboid	Diameter of the cylinder
3	Cylinder	Cuboid	Diameter of the cylinder	Length of the square base of the cuboid
4	Cuboid	Cuboid	Length of the square base of the cuboid	Length of the square base of the cuboid
5	Cylinder	Sphere	Diameter of the cylinder	Diameter of the sphere
6	Cuboid	Sphere	Length of the square base of the cuboid	Diameter of the sphere

The dimensions of HRs are chosen in order to be sufficiently big to avoid manufacturing issues, while also being sufficiently small to preserve their interest in terms of acoustic applicability in the fields of transport engineering (e.g.: aerospace, automotive, etc.). More specifically, the neck and cavity dimensions are reported in Table 2. In detail, d_{cavity} always depends on d_{neck} by the parametric value ξ, which is varied from 0.05 to 0.95 with a step of 0.05. Thanks to this, 114 different geometrical configuration are numerically studied.

Table 2 Dimensions of neck and cavity for each configuration

C.	d_{neck} [mm]	l_{neck} [mm]	d_{cavity} [mm]	l_{cavity} [mm]	ξ
1	4	5	d_{neck}/ξ	25	0.05:0.05:0.95
2	5	5	d_{neck}/ξ	25	0.05:0.05:0.95
3	5	4	d_{neck}/ξ	35	0.05:0.05:0.95
4	5	4	d_{neck}/ξ	35	0.05:0.05:0.95
5	4	30	d_{neck}/ξ	d_{neck}/ξ	0.05:0.05:0.95
6	4	30	d_{neck}/ξ	d_{neck}/ξ	0.05:0.05:0.95

2.2 Finite element implementation

For what concerns the FE implementation, the module "Pressure Acoustics, Frequency Domain" of COMSOL MultiPhysics is used both as modeling tool and numerical solver. For all configurations presented in this work, the mesh consists of tetrahedral elements generated through physics-controlled algorithms that are pre-implemented in the software. Nevertheless, the authors verified that the maximum element size of each HR meshed is always lower then 1/6 of the minimum wavelength λ; in practice, for each configuration, the maximum tunable frequency of the studied Helmholtz Resonators is limited by its minimum wavelength, which in any case must be greater than the dimension of six elements of the model, as recommended in literature [28]. In Table 3, the average number of FE mesh elements for each of the studied configurations are reported.

The analyzed HRs are filled by air, whose properties are: density $\rho_0 = 1.225$ [kg/m^3], speed of sound $c_0 = 343$ [m/s]. The forced-response analyses are carried out considering an excitation of 1Pa over the free end of the neck, while the HR walls are modeled through Sound Hard Boundary Wall (SHBW) conditions, which means that the normal component of the acceleration (and thus the velocity) is zero. A detailed description of classical FE formulation and equations can be easily found in the context of the relevant literature [29].

3 Polynomial fitting of Helmholtz resonances

In this section, the six configurations previously defined are studied, and some results are presented as functions of the ratio ξ. Present numerical results are already well described in the research presented at the CEAS Aerospace Europe Conference 2021 by Catapane et al. [23]; graphical and polynomial approximation is limiting for several reasons, well explained in Sub-Section 3.2. Even though the numerical campaign is updated and improved respect to the above-mentioned work, the scope of the present study is to depict limits of a graphical/polynomial approach for tuning the resonance frequency of a Helmholtz Resonator, and to overcome them with a new semi-analytical investigation (Sect. 4).

Table 3 Average number of FE mesh elements

Configuration	Domain	Boundary	Edge
1	5652	1130	149
2	3021	682	114
3	5846	985	127
4	6731	1044	133
5	2828	656	116
6	3007	702	125

3.1 Development of graphical and polynomial approaches for the correction factor estimation

A FE parametric test campaign is carried out with the aim to estimate the resonance frequency of HRs for *Configurations 1 - 6*, varying the main neck-cavity length ratios ξ from 0.05 to 0.95. Starting from this set of data, Eq. 8 is inverted and f_{res} is set to $f_{res(FEM)}$ to obtain the value of the correction factor $c_{f(FE)}$ as:

$$c_{f(FE)} = \left(\frac{c_0^2}{4\pi^2} \frac{S_{neck}}{f_{res(FE)}^2 V_{cavity} l_{neck}} - 1 \right) \xi^{-1}. \tag{9}$$

Such values of the correction factor are shown in Fig. 2a). It may be interesting to notice that, for all the analyzed configurations, in the range $0.05 < \xi < 0.3$ the values of $c_{f(FE)}$ sharply change with a descending pattern, while increasing smoothly in the range $0.3 < \xi < 0.95$. In addition, the Rayleigh formulation of Eq. 7 works consistently up to $\xi = 0.3$, but its prediction is not anymore acceptable for $\xi > 0.3$, as it is possible to see in Fig. 2b), which shows the values of $100 \cdot \left| \frac{f_{res(Rayleigh)} - f_{res(FE)}}{f_{res(FE)}} \right|$, confirming the limitations of the problem concerning Helmholtz resonance frequency estimation through Eq. 7. These almost coincident ranges can be interpreted in a very simple way just taking into account Eq. 7: in the first range, the effective length is adjusted just with the neck diameter, and it works well because the cavity section area is quite bigger than the neck one. In that region, the correction factor can be evaluated ignoring the geometry of the cavity, and hence neglecting the influence of ξ. On the other hand, when the cavity section area is comparable with the neck one, Eq. 7 it is not anymore valid and the correction factor must be evaluated in a different way. Fig. 2a) may be intended as a carpet plot, in which the potential user may enter with a designed value of ξ, choose the appropriate curve according to the considered geometry, and obtain a value of c_f that can be used in Eq. 8 in order to predict the resonance frequency of a specific HR device.

With the objective of developing an alternative approach to the graphical estimation of the correction factor c_f, and consequently of the HR frequency f_{res}, a 3rd-order polynomial approximation of the correction factors is proposed herein. Since Rayleigh's formula reported in Eq. 7 performs for ratios $0.05 < \xi < 0.3$ with a level of accuracy that is definitely acceptable, and considering that, as already underlined, in the range $0.05 < \xi < 0.3$ the values of c_f vary meaningfully, while changing less in the range $0.3 < \xi < 0.95$,

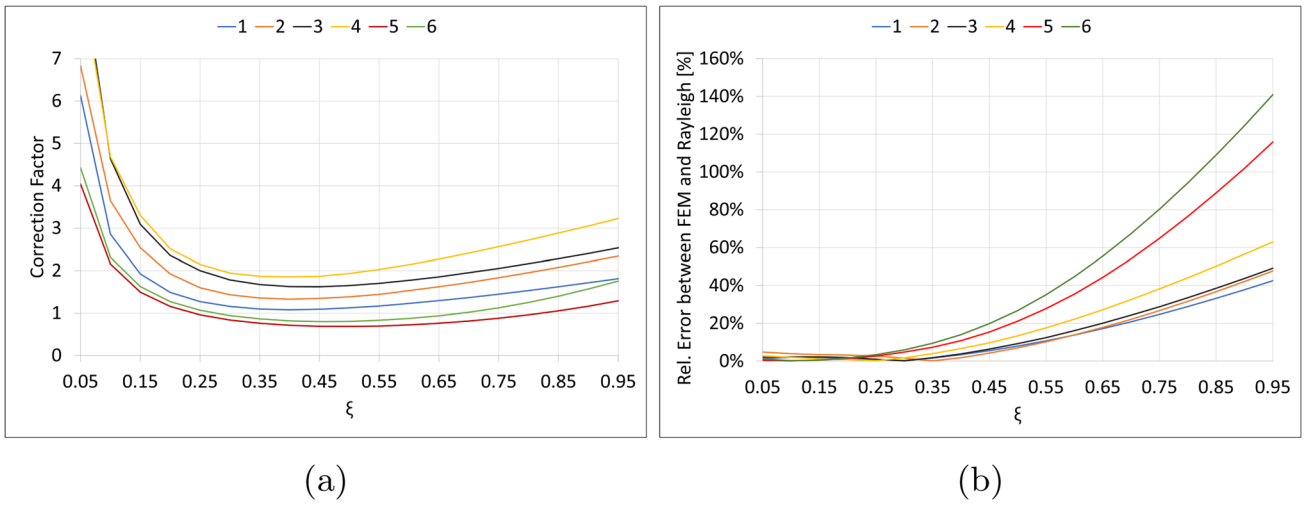

Fig. 2 **a** FE estimation of the correction factor for the six studied HR configurations, as functions of ξ; **b** Evaluation of the relative errors of Rayleigh's formula, with reference to Finite Element results, for the six studied HR configurations, as functions of ξ

then it may be convenient to directly rely on Eq. 7 up to $\xi = 0.3$, and to contextually develop a polynomial approximation for higher values of ξ.

As it may be noticed from Fig. 3, which shows the HR frequencies of the six studied configurations, for $0.05 < \xi < 0.3$ Rayleigh's formula is always able to catch the FE behavior with a negligible accuracy error, while for $\xi > 0.3$ the proposed 3rd-order polynomial approximations almost perfectly follow FE values, with a maximum relative error respect to the FE values not greater than 2%. Clearly, if one wants to derive a polynomial expression with reasonable validity in the whole ξ range, a higher-order polynomial would be needed. The above-mentioned polynomial expressions are derived using MATLAB's built-in *polyfit* function and are meant to be used in Eq. (8) with the aim of mathematically calculating the resonance frequency of a HR. The expressions that refer to *Configurations 1 - 6* are reported in Eq. 10.

$$\begin{aligned}
c_{f(poly,1)} &= -3.72\xi^3 + 9.31\xi^2 - 5.89\xi + 2.20,\\
c_{f(poly,2)} &= -5.16\xi^3 + 12.9\xi^2 - 8.20\xi + 2.89,\\
c_{f(poly,3)} &= -5.98\xi^3 + 14.8\xi^2 - 9.75\xi + 3.60,\\
c_{f(poly,4)} &= -6.79\xi^3 + 16.7\xi^2 - 10.2\xi + 3.73,\\
c_{f(poly,5)} &= -0.30\xi^3 + 6.49\xi^2 - 2.18\xi + 0.60,\\
c_{f(poly,6)} &= -0.26\xi^3 + 8.18\xi^2 - 2.52\xi + 0.65.
\end{aligned} \tag{10}$$

3.2 Limitations of the graphical and polynomial approaches

Previous results are an update of the work submitted and presented at the CEAS Aerospace Europe Conference 2021 by Catapane et Al. [23]. In detail, the previous work considered sphere, cylinder and cube as main geometries, which are combined in a reasonable way to design *Configurations 1 - 6*; the study was carried out by varying the geometric properties of the cavity without regarding the resonance frequency, thus resulting in a frequency range that was much wider than that which is actually interesting for industrial application. In the present work, as it is possible to see in Fig. 3, the maximum resonance frequency is always below 3000Hz; therefore, each analyzed HR can be used for a real low-frequency application, since at higher frequencies a tonal solution would not be as efficient as a foam (e.g.: melamine, polyurethane). Furthermore, *Configurations 3 - 4* presented in the conference paper [23] showed an anomalous trend: FEM resonance frequency is always coincident with Rayleigh prediction (Fig. 4). These results are not trivial to motivate, but the geometry has a strong influence on the results: *Configurations 3 - 4* are made with cubic cavity, which lead to a Correction Factor not dependent by any geometric property of the Helmholtz Resonator. This is valid just for an exactly cubic cavity, and it is a specific result that will be demonstrated in next section with the new semi-analytical approach (Sect. 4). In the end, the cubic geometries are replaced by cuboid cavities, in order to provide more general results. Thanks to Figs. 2 and 3, it is possible to understand that Rayleigh formulation is not always valid, and extended geometrical considerations must be done in the design phase of an Helmholtz Resonator. The pattern of Correction Factor is almost similar for each configuration, which leads to the consideration that an absolute evaluation, regardless of the primitives and the geometrical ratios, is feasible. The applications of such approach are reasonably bounded by industrial applications and manufacturing

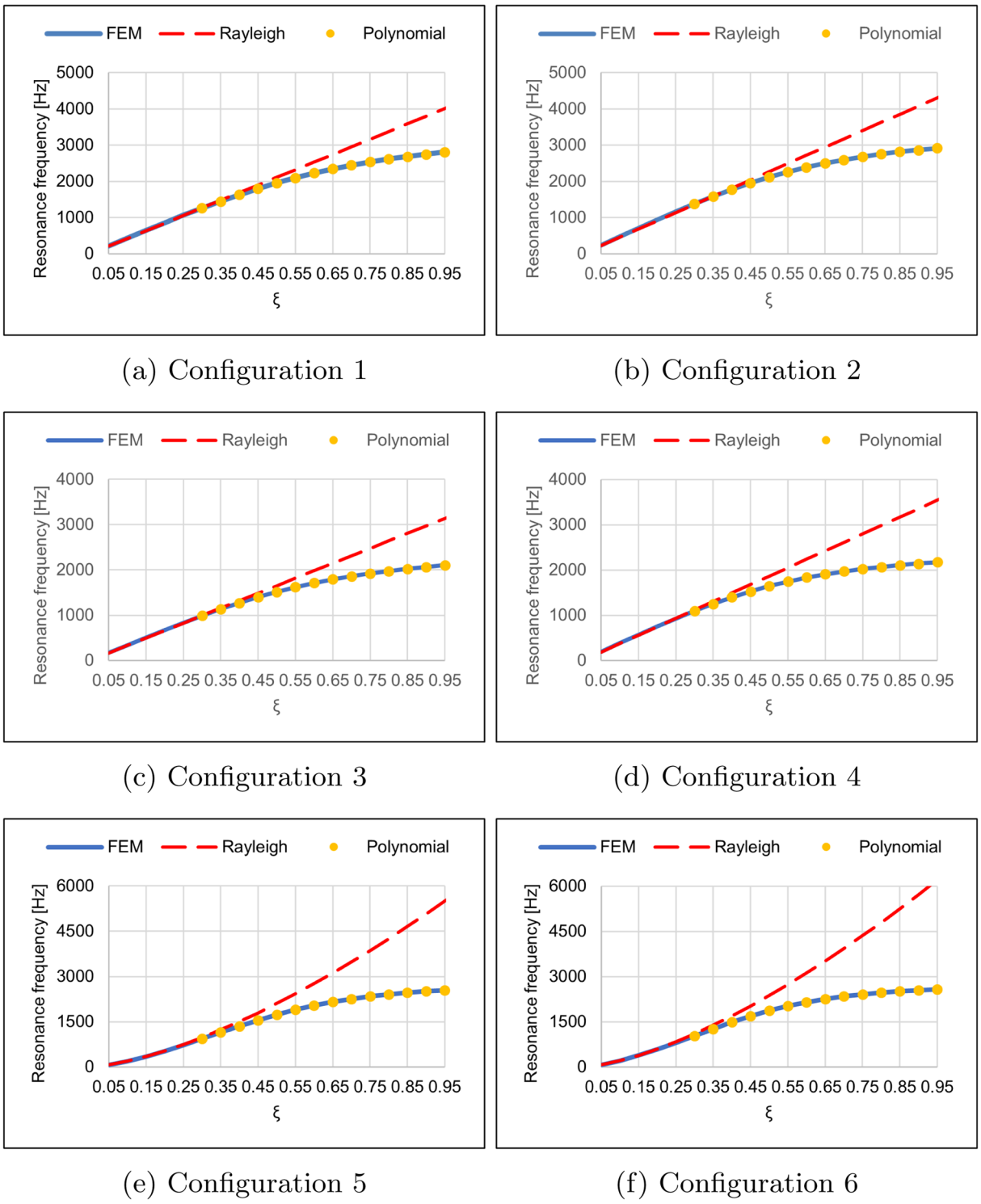

Fig. 3 Comparison of Helmholtz resonance frequency estimations for each analyzed configuration

issues; nevertheless, a graphical and polynomial approximation is affected by scalability problem. Furthermore, the current approach is based on the assumption that the correction factor depends on the ratio between d_{neck} and d_{cavity}, according to Ingard intuition [27], but it cannot be excluded that other parameters, such as l_{neck} and l_{cavity} may have considerable effects.

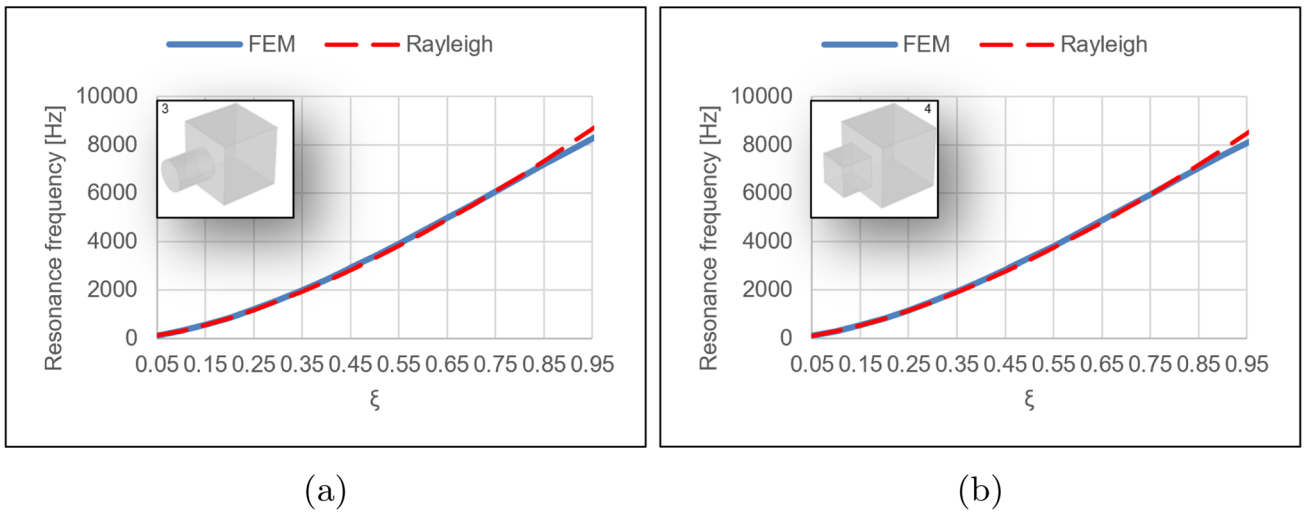

Fig. 4 Comparison between Helmholtz resonance frequencies evaluated with Rayleigh formulas for *Configurations 3 and 4* with a perfect cubic cavity [23]

4 Semi-analytical estimation of scalable Helmholtz resonances

As well explained in previous section, graphical and polynomial estimations are not exact solutions and can be affected by scaling problems. This leads to the necessity to find an exact method, which does not depend on specific dimensions: the semi-analytical approach proposed herein is able to overcome this limit for two different configurations. This approach has been developed taking into account that, after 3000Hz, a tonal solution cannot be competitive with foams, and Helmholtz resonator thickness dimensions ($L_{neck} + L_{cavity}$) are not bigger than 10cm. With these maximum dimensions, an acoustic resonator studied herein can be designed and applied for a transport engineering application, even for aeronautical applications, where space limitations are severe and difficult to match with performance.

4.1 Methodological framework

The following method is based on the resonance frequency properties of tonal sources like Helmholtz resonators and Quarter Wavelength Tubes (QWT). Previous sections are very useful to understand how strong the correction factor may affect the resonance frequency of HRs, and that its value cannot be assumed only as a function of neck dimensions. The correction factor must depend on ξ, defined as the ratio between the representative lengths in the section plane of the neck and the cavity, respectively labeled as d_{neck} and d_{cavity}. It is possible to notice that for $\xi = 1$, $d_{neck} = d_{cavity}$; this means that for neck and cavity with same geometry, the Helmholtz Resonator becomes a tube with constant section area. In detail, *Configuration 1* and *4*, respectively Cylinder neck - Cylinder cavity and Cuboid neck - Cuboid cavity, show the above-described behavior (Fig. 1). A tube with constant section area has specific resonance frequencies when the tube length is an odd-integer multiple m of the quarter of the wavelength [24]. Therefore, such a system reaches its maximum absorption when the exciting frequency is equal to one of its resonance frequencies, expressed as:

$$f_{QWT} = \frac{(2m-1)c}{4L}. \tag{11}$$

where L is the length of the tube, and in this case is $L = L_{neck} + L_{cavity}$ when $\xi = 1$. Hence, it is straightforward that Helmholtz resonance frequencies of *Configuration 1* and *4* when $\xi = 1$ should be equal to the first ($m = 1$) QWT resonance:

$$\frac{c_0}{4L} = \frac{c_0}{2\pi}\sqrt{\frac{S_{neck}}{V_{cavity} l_{neck}(1+c_f)}}. \tag{12}$$

With regards to *Configuration 1* and *4*,

$$S_{neck}/V_{cavity} = D_{neck}^2/D_{cavity}^2 L_{cavity} = \xi^2/L_{cavity} = 1/L_{cavity}, \tag{13}$$

thus, the equivalence can be written as:

$$\frac{c_0}{4(L_{neck}+L_{cavity})} = \frac{c_0}{2\pi}\sqrt{\frac{1}{L_{cavity} L_{neck}(1+c_f)}}. \tag{14}$$

Since the correction factor (c_f) is the only unknown term, it is possible to analytically derive it as:

$$c_f = \frac{4}{\pi^2}\frac{(L_{neck}+L_{cavity})^2}{L_{cavity}L_{neck}} - 1. \tag{15}$$

A new correction factor formula is obtained: QWT formula is used as a boundary condition, leading to an analytical formulation of the correction factor which depends just on the geometric properties of the Helmholtz Resonator. Furthermore, Eq. 15 can be used even for *Configuration 4*, where $D_{neck} = L_{neck}$ and $D_{cavity} = L_{cavity}$; with few algebraic calculations, the correction factor for *Cube - Cube Configuration* is:

$$c_{f(Cube-Cube)} = \frac{16}{\pi^2} - 1, \tag{16}$$

which does not depend on any geometrical property; due to this reason, as it is possible to see from Fig. 4, the previous *Configuration 4* [23] had an anomalous trend: in the case of *Cube - Cube Configuration*, the correction factor is constant respect to any change in length.

4.2 Results and discussion

Fig. 5 aids to comprehend the physics of the problem: considering FE results as reference, it is clear that Rayleigh formula works well for low ξ values, but it is not consistent where the section area dimension of the neck is comparable with the section area dimension of the cavity. In particular, FE results are coherent with the assumption done in the previous section, since their resonance frequency at $\xi = 1$ matches perfectly the QWT resonance frequency: the FE curve asymptotically tends to the QWT resonance frequency, actually reaching it at $\xi = 1$.

The semi-analytical curve is developed considering Eq. 8, with a slight change motivated by the fact that it has been empirically verified that the effective length depends on the second power of the ratio ξ, rather than on the first one (Fig. 6):

$$f_{res(\xi^2)} = \frac{c_0}{2\pi}\sqrt{\frac{S_{neck}}{V_{cavity}l_{neck}(1+c_f\xi^2)}}, \tag{17}$$

Indeed, the equivalent FE results correction factor, evaluated with Eq. 9, is very similar to Rayleigh's $c_{f(Rayleigh)}$ up to $\xi \approx 0.3$ and then it follows asymptotically the line related to the proposed approach of equation $c_f \cdot \xi$.

It is noteworthy to highlight the difference between the Rayleigh c_f (Eq. 5), the graphical-polynomial c_f (Eq. 9) and new c_f of Eq. 15. Indeed, the Rayleigh c_f depends on the radius of the neck, the FE c_f depends on the ratio of the main dimension of the section area of the neck and the one of the cavity ξ, leading to the essential observation that other geometrical parameters are not considered for the correction factor estimation; as mentioned in Sect. 3.2, this can be one of the main limit of the graphical-polynomial approach. With regard to Eq. 17, where semi-analytical correction factor is firstly inserted, there is a correction factor which depends on L_{neck} and L_{cavity}, multiplied by ξ^2 which is $(d_{neck}/d_{cavity})^2$. Hence herein every geometrical parameter is taken into account and can affect the effective length that should be inserted in the resonance frequency. It is straightforward to define the new semi-analytical

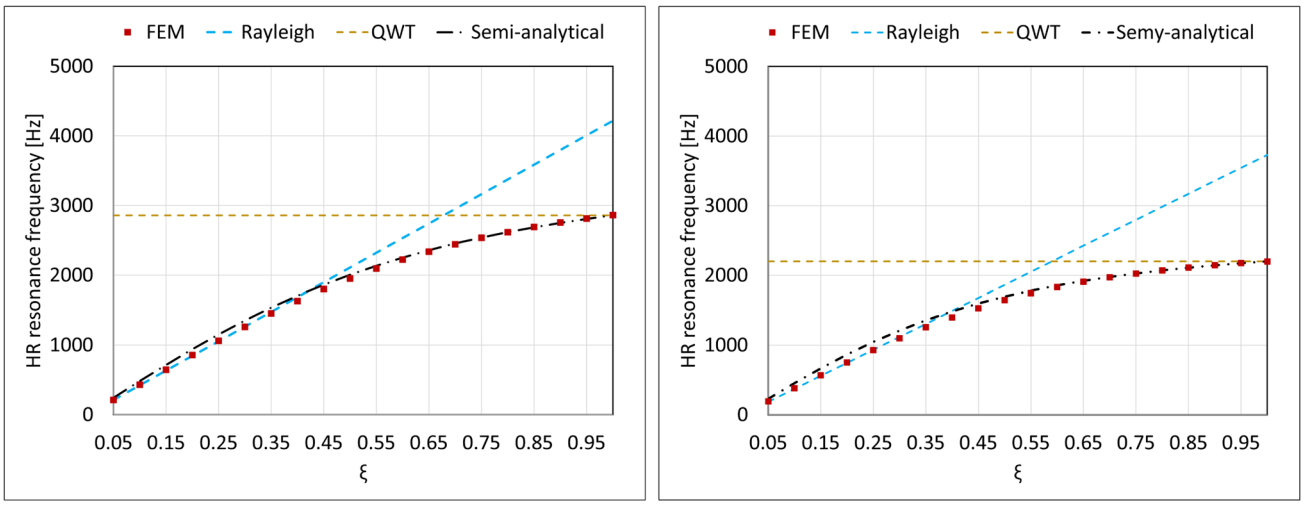

(a) Configuration 1 (b) Configuration 4

Fig. 5 Comparison between Helmholtz resonance frequencies evaluated with FEM, Rayleigh, QWT formulas and the new semi-analytical approach for *Configurations 1* and *4*

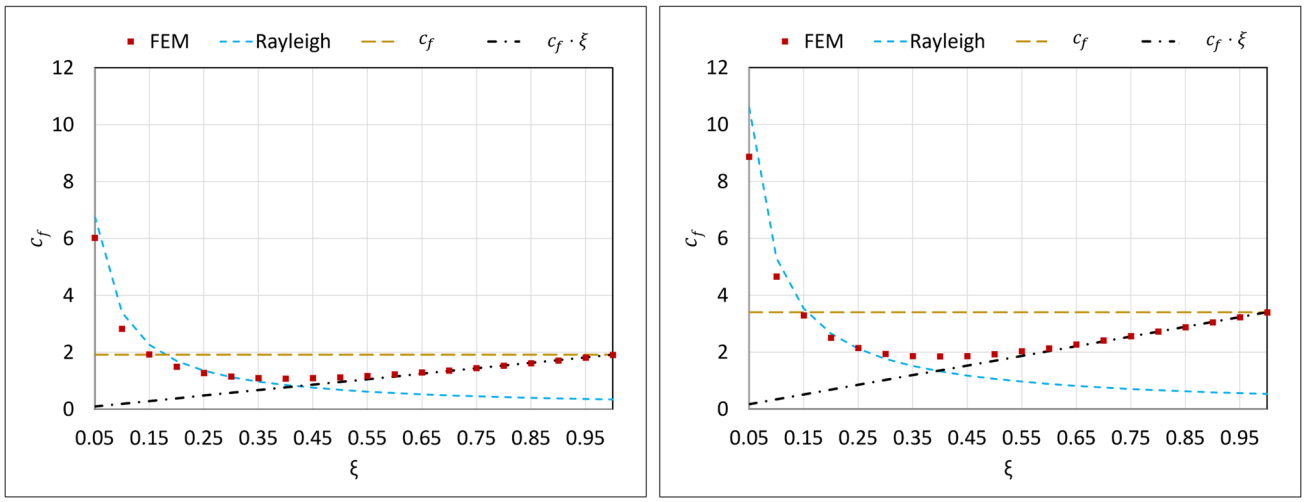

(a) Configuration 1 (b) Configuration 4

Fig. 6 Comparison between the correction factor c_f derived by FE results through Eq. 9, by Rayleigh through Eq. 8, and c_f evaluated thanks to Eq. 15 for *Configurations 1* and *4*. The line of equation $c_f \cdot \xi$ is useful for the formulation of Eq. 17; again, c_f is evaluated thanks to Eq. 15

formulation as more complete respect to previous ones. Furthermore, comparing the Rayleigh formulation with the new one, it is possible to define a ξ range where there is just a strong dependency on the main dimension of section area of the neck, and a ξ region where each geometrical parameter must be taken into account for the correct evaluation of the correction factor. Indeed, even though the semi-analytical curves seem to be completely representative of the FE results in the overall range of ξ, it is noticed that the relative error of the semi-analytical approach is bigger than Rayleigh's one for low values of ξ (Fig. 7).

Thus, a concrete possibility is to weight the two formulas and definitively states a correction factor formula for an Helmholtz resonator, which has no limits in terms of dimensions.

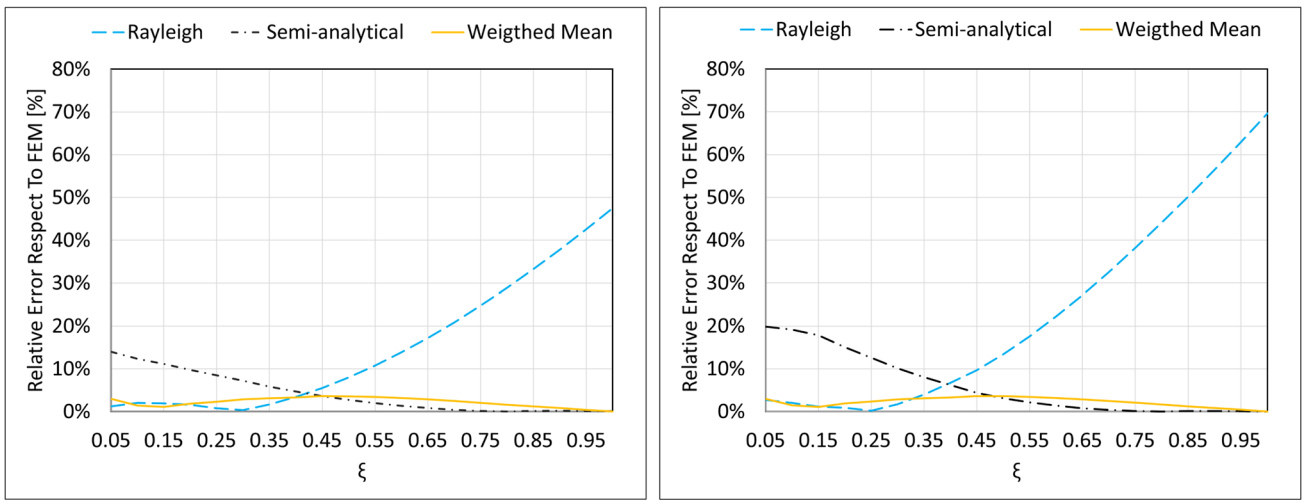

(a) Configuration 1 (b) Configuration 4

Fig. 7 Comparison between relative errors of the Rayleigh formula (Eq. 7), the semi-analytical approach (Eq. 17) and the resonance frequency derived through general resonance equation (Eq. 7), with c_f taken by Eq. 18 respect to FE results for *Configurations 1* and *4*

$$c_{f(WM)} = \frac{(1-\xi^2)\cdot\left[\frac{4}{3\pi}\frac{d_{cavity}}{l_{neck}}\right] + \xi^2\cdot\left[\frac{4}{\pi^2}\frac{(L_{neck}+L_{cavity})^2}{L_{cavity}L_{neck}} - 1\right]}{\xi^2}. \tag{18}$$

The weighted mean can be inserted in the resonance frequency formula in Eq. 17, when the primitive geometry of the neck is coincident with the one of the cavity; with this formula, the Helmholtz resonance prediction problem is solved with high accuracy and without polynomial or graphical predictions, which are surely useful but not comparable with a semi-analytical approach. In detail, the maximum relative error is about 3% for Configuration 1 and 5% for Configuration 4; both maximum relative errors are reached in correspondence of a ξ-value between 0.4 and 0.5, as it is possible to see through Fig. 7. It is reasonable that the maximum error is in that range of ξ, because Rayleigh formula works well for lower value of ξ, and Eq. 15 works perfectly while ξ tends to 1. On the other hand, Eq. 7 and Eq. 15 can be used respectively when ξ is closer to 0 and when ξ is approximately greater than 0.5.

5 Conclusions

The present work aims at obtaining an accurate prediction of the tuning frequency of Helmholtz-resonating devices, in order to design tonal devices for acoustic applications. To this scope, it is performed an investigation on a correction factor for the classical formulation used to estimate the Helmholtz resonance frequency starting from its geometric characteristics, in the case of different-shaped resonators with varying neck-cavity ratios. In detail, a set of Finite Element analyses are carried out, and results in terms of correction factors are firstly provided in both graphical and polynomial form, also demonstrating that the original formulation is not exhaustive for the precise design of an Helmholtz Resonator. Moreover, results in terms of correction factors, resonance frequencies and relative errors are provided and discussed. Once explained the limits of both graphical and polynomial approaches, a semi-analytical method is proposed, and relative results are plotted and motivated. With this method, it is possible to overcome limits of graphical and polynomial approaches in the case of specific geometries. With reference to different neck- cavity geometric couplings, the polynomial and graphical estimations are still preferred compared to Rayleigh formulation. On the base of the current results, future research can be centered on the development of a semi-analytical method which could be generalized for each geometric configuration, as well as it may take into account the effects of the wall material.

Acknowledgements The authors acknowledge the support of the Italian Ministry of Education, University and Research (MIUR) through the project DEVISU, funded under the scheme PRIN-2107 - grant agreement No. 22017ZX9X4K006.

Funding Open access funding provided by Università degli Studi di Napoli Federico II within the CRUI-CARE Agreement.

References

1. Magliacano, D., Petrone, G., Franco, F., De Rosa, S.: Numerical investigations about the sound transmission loss of a fuselage panel section with embedded periodic foams. Appl. Acoust. (2021). https://doi.org/10.1016/j.apacoust.2021.108265
2. Catapane, G., Magliacano, D., Petrone, G., Casaburo, A., Franco, F., De Rosa, S.: Transmission loss analyses on different angular distributions of periodic inclusions in a porous layer. Aerotecnica Missili e Spazio (2021). https://doi.org/10.1007/s42496-021-00101-6
3. Tang, Y., Ren, S., Meng, H., Xin, F., Huang, L., Chen, T., Zhang, C., Lu, T.J.: Hybrid acoustic metamaterial as super absorber for broadband low-frequency sound. Sci. Rep. (2017). https://doi.org/10.1038/srep43340
4. Magliacano, D., Ciminello, M., Dimino, I., Viscardi, M., Concilio, A.: Active vibration control of a mounting bracket for automotive gearboxes. Int. J. Mech Eng **1**, 69–74 (2016)
5. Magliacano, D., Ahsani, s., Ouisse, M., Deckers, E., Petrone, G., Desmet, W., De Rosa, S.: Formulation and validation of the shift cell technique for acoustic applications of poro-elastic materials described by the Biot theory. Mechanical Systems and Signal Processing **147** (2020). https://doi.org/10.1016/j.ymssp.2020.107089
6. Casaburo, A., Magliacano, D., Petrone, G., Franco, F., De Rosa, S.: Gaussian-based machine learning algorithm for the design and characterization of a porous meta-material for acoustic applications. Appl. Sci. (2022). https://doi.org/10.3390/app12010333
7. Thompson, M.P., Engleman, H.W.: The two types of resonance in intake tuning. American Society of Mechanical Engineers, vol. 1, pp. 1–8 (1969)
8. Driels, M.R.: Dynamics of i. c. engine induction systems. Journal of Sound and Vibration 43(3), 499–510 (1975). https://doi.org/10.1016/0022-460X(75)90003-6
9. Jameson, R.T., Hodgins, P.A.: Improvement of the torque characteristics of a small, high-speed engine through the design of Helmholtz-tuned manifolding. SAE International (1990). https://doi.org/10.4271/900680
10. Mekid, S., Farooqui, M.: Design of Helmholtz resonators in one and two degrees of freedom for noise attenuation in pipe lines. Acoust. Aust. **40**, 194–202 (2012)
11. Gorny, L., Kooopmann, G., Neise, W., Lemke, O.: Attenuation of Ducted Axial Propulsors' Blade Tone Noise Using Adaptively Tunable Resonators. https://doi.org/10.2514/6.2007-3529

12. Zhao, D., Morgans, A.S.: Tuned passive control of combustion instabilities using multiple Helmholtz resonators. J. Sound Vib. **320**, 744–757 (2009). https://doi.org/10.1016/j.jsv.2008.09.006
13. Alster, M.: Improved calculation of resonant frequencies of Helmholtz resonators. J. Sound Vib. **24**(1), 63–85 (1972). https://doi.org/10.1016/0022-460X(72)90123-X
14. Kinsler, L.E., Frey, A.R., Coppens, A.B., Sanders, J.V.: Fundamentals of acoustics, Fourth Edition, pp. 284–285 (2000)
15. Tang, P.K., Sirignano, W.A.: Theory of a generalized Helmholtz resonator. J. Sound Vib. **26**(2), 247–262 (1973). https://doi.org/10.1016/S0022-460X(73)80234-2
16. Fahy, F.J., Schofield, C.: A note on the interaction between a Helmholtz resonator and an acoustic mode of an enclosure. J. Sound Vib. **72**, 365–378 (1980). https://doi.org/10.1016/0022-460X(80)90383-1
17. Chanaud, R.C.: Effects of geometry on the resonance frequency of Helmholtz resonators. J. Sound Vib. **178**(3), 337–348 (1994). https://doi.org/10.1006/jsvi.1994.1490
18. De Bedout, J., Franchek, M., Bernhard, R., Mongeau, L.: Adaptive-passive noise control with self-tuning Helmholtz resonators. J. Sound Vib. **202**(1), 109–123 (1997). https://doi.org/10.1006/jsvi.1996.0796
19. Lei, G.T., Techentin, R.W., Gilbert, B.K.: High-frequency characterization of power/ground-plane structures. IEEE Trans. Microw. Theory Tech. **47**, 562–569 (1999). https://doi.org/10.1109/22.763156
20. Griffin, S., Lane, S.A., Huybrechts, S.: Coupled Helmholtz resonators for acoustic attenuation. J. Vib. Acoust. **123**(1), 11–17 (2000). https://doi.org/10.1115/1.1320812
21. Tang, S.K.: On Helmholtz resonators with tapered necks. J. Sound Vib. **279**(3), 1085–1096 (2005). https://doi.org/10.1016/j.jsv.2003.11.032
22. Park, S.-H.: Acoustic properties of micro-perforated panel absorbers backed by Helmholtz resonators for the improvement of low-frequency sound absorption. J. Sound Vib. **332**, 4895–4911 (2013). https://doi.org/10.1016/j.jsv.2013.04.029
23. Catapane, G., Magliacano, D., Petrone, G., Casaburo, A., Franco, F., De Rosa, S.: Evaluation of improved correction factors for the prediction of Helmholtz resonances. Proceedings of CEAS Aerospace Europe 2021 Conference, Warsaw, Poland **1** (2021)
24. Long, M.: Architectural acoustics, (2006)
25. Rayleigh, J.W.S.: The theory of sound, (1898)
26. Karal, F.C.: The analogous acoustical impedance for discontinuities and constrictions of circular cross section. J. Acoust. Soc. Am. **25**(2), 327–334 (1953). https://doi.org/10.1121/1.1907041
27. Ingard, U.: On the theory and design of acoustic resonators. J. Acoust. Soc. Am. **25**(6), 1037–1061 (1953). https://doi.org/10.1121/1.1907235
28. Mace, B.R., Manconi, E.: Modelling wave propagation in two-dimensional structures using finite element analysis. J. Sound Vib. (2008). https://doi.org/10.1016/j.jsv.2008.04.039
29. Isaac, C., Wrona, S., Pawełczyk, M., Roozen, N.B.: Numerical investigation of the vibro-acoustic response of functionally graded lightweight square panel at low and mid-frequency regions. Composite Struct. (2021). https://doi.org/10.1016/j.compstruct.2020.113460